Original Article

Dosimetric comparisons of craniospinal axis irradiation using helical tomotherapy, volume-modulated arc therapy and intensity-modulated radiotherapy for medulloblastoma

Yangqing Sun, Gui Liu, Wen Chen, Taili Chen, Pei Liu, Qian Zeng, Jidong Hong, Rui Wei

Department of Oncology, Xiangya Hospital, Central South University, Changsha 410008, China

Contributions: (I) Conception and design: Y Sun, R Wei; (II) Administrative support: R Wei; (III) Provision of study materials or patients: R Wei, G Liu, T Chen; (IV) Collection and assembly of data: Y Sun, W Chen, P Liu, Q Zeng; (V) Data analysis and interpretation: Y Sun, W Chen; (VI) Manuscript writing: All authors; (VII) Final approval of manuscript: All authors.

Correspondence to: Rui Wei. Department of Oncology, Xiangya Hospital, Central South University, Changsha 410008, China. Email: weiruix@163.com.

Background: To evaluate the potential dosimetric gains of helical tomotherapy (HT) versus intensity-modulated radiotherapy (IMRT) and volume-modulated arc therapy (VMAT) for craniospinal axis irradiation (CSI) of medulloblastoma.

Methods: A total of 36 treatment plans were calculated retrospectively for 12 patients with medulloblastoma receiving CSI using HT with TomoTherapy Hi-Art Software (Version 2.0.7) (Accuray, Madison, WI, USA). For each case, the other two different delivery techniques were re-planned with IMRT/VMAT optimized with Eclipse treatment planning system (TPS) (Version 11.0.31). Homogeneity index (HI) and conformity index (CI) of the planning target volume (PTV) and organs at risk (OARs) sparing were analyzed. Differences in plans were evaluated using paired-samples *t*-test for various dosimetric parameters.

Results: HT yielded the highest CI in all PTV coverage including PTV of gross tumor volume (PGTV) (HT: 0.7163; VMAT: 0.6688; IMRT: 0.6096), PTVbrain (HT: 0.8490; VMAT: 0.8384; IMRT: 0.7815) and PTVspine (HT: 0.5904; VMAT: 0.5862; IMRT: 0.5797). Meanwhile, HT yielded better HI in PGTV (HT: 0.0543; VMAT: 0.0759; IMRT: 0.0736), PTVbrain (HT: 0.5525; VMAT: 0.5619; IMRT: 0.5554) and PTVspine (HT: 0.0700; VMAT: 0.0782; IMRT: 0.0877). As for OARs, HT demonstrated marked superiority in critical organs including maximal/mean doses of brainstem PRV, optical chiasm and optic nerves.

Conclusions: For CSI of medulloblastoma, HT offers superior outcomes in terms of PTV conformity, PTV homogeneity and critical OAR sparing as compared with IMRT/VMAT.

Keywords: Craniospinal axis irradiation treatment (CSI treatment); medulloblastoma; dosimetric comparison; intensity-modulated radiotherapy (IMRT); volume-modulated arc therapy (VMAT); helical tomotherapy (HT)

Submitted Oct 08, 2018. Accepted for publication Jan 15, 2019.
doi: 10.21037/tcr.2019.01.30
View this article at: http://dx.doi.org/10.21037/tcr.2019.01.30

Introduction

As one of the primitive neuroectodermal tumors of the cranium (PNETs), medulloblastoma is fairly common among pediatric brain malignancies, yet rare in adults. The extreme invasiveness and strong inclination of cerebrospinal fluid (CSF) dissemination (1) may explain its high level of malignancy. At present, adjuvant craniospinal axis irradiation (CSI) is a standard postoperative treatment (2).

With the rapid developments in radiation physics, computer technology, treatment planning systems (TPS) and linear accelerator delivery capabilities, many new radiotherapeutic techniques, including intensity-modulated radiation therapy (IMRT), volumetric-modulated radiation therapy (VMAT) and helical tomotherapy (HT), have emerged and improved dose distribution in planning target volume (PTV) coverage and treatment efficiency (3,4).

Table 1 Patient demographics

Characteristics	n
Age, years	
<18	6
≥18	6
Median age	16
Sex	
Male	8
Female	4
Volume of gross tumor, cm^3	
Mean	14.3
Maximum	32.8
Minimum	5.9

Radiation dose might be optimized through variable intensity beams (5). Pioneered in 1993, IMRT obtains the shape of the radiation field in accordance with the projective shape of PTV in radiation beam direction. Thus, multiple fixed angle radiation beams are usually required for better qualities. In addition, the technology offers the ability to produce concavities in the treatment volume to improve conformality (6), which can greatly improve patients' quality of life (7-9). Nevertheless, exceedingly prolonged delivery time and monitor units (MUs) along with conventional conformal radiotherapy (CRT) can decrease efficiency and lead to more intrafraction setup errors during treatment (10,11). Some concerns have persisted, namely that large MUs can increase the risks of secondary radiation-induced malignancies due to incremental scattered radiation and low-dose radiation to the rest of the body (12).

Arc-based or rotational therapies have come into existence to overcome the above inherent drawbacks of large MUs in IMRT. VMAT may achieve precise conformal dose distribution via the variability of multi-leaf collimator (MLC) position, dose rate and gantry rotation speed with a continuous rotation of the radiation source from a full 360° beam angle (13). Furthermore, in one study, the reduction of treatment delivery time was revealed to be more dramatic in MUs (14).

Based upon spiral computed tomography (CT), Hi-Art HT serves as an imaging guide for improving therapeutic accuracy. A 6 MV linear accelerator delivers radiation in a fan-shaped distribution. While the treatment couch moves along an axis, rotatory radiation is delivered to realize a full 360° direction of the radiation beam. This unique motion allows for a maximal distance of 160 cm. With a broader field of irradiation, it overcomes the defects of cold points and out-of-range junctions using IMRT/VMAT. Based on refined adjustments and better controls, HT theoretically offers higher dosage conformity and lower doses to adjacent OARs than IMRT. However, a certain number of MUs and ample treatment time are still required.

Over the last decade, dosimetric comparison among HT, IMRT, and VMAT have been widely explored for malignant head-and-neck, thoracic and abdominal tumors. Few literature studies have applied these techniques to medulloblastoma. Here, the authors compared the dosimetric advantages and disadvantages of IMRT, VMAT, and HT for patients on CSI to provide a reference for clinical practices.

Methods

Patient characteristics

A total of 12 newly histologically diagnosed intracranial medulloblastoma patients having received CSI using the HT system from October 2015 to October 2017 were recruited from the Department of Oncological Radiotherapy, Xiangya Hospital, Central South University. The scanning datasets of enhanced CT were prospectively maintained. All patients received routine pretreatment evaluations, including complete physical examination, Karnofsky performance status (KPS) scoring, hematological & biochemical panels, electrocardiogram, chest radiography and ultrasonography of the whole abdomen. No patients had distant metastases. Without preoperative chemoradiotherapy, they were operated on one month earlier. Their clinical characteristics are summarized onin *Table 1*. According to clinical risk stratification that high-risk criteria including non-infant (>3 years) patients, residual tumor at primary site >1.5 cm^2, metastatic dissemination, or large-cell/anaplastic hypotype, we divided all the patients into the average risk group and the high risk group. The risk stratification of these patients, along with the dose of CSI they received, is summarized in *Table 2*.

Treatment planning

With arms resting at both sides, the subjects were positioned supinely and immobilized on a scanning bed with an EFFCAST thermoplastic head-neck-shoulder mask. Body marker lines were also made for fixation. They were

Table 2 Risk stratification and prescribed doses

Risk stratification	n	Prescribed doses [total doses (Gy)]		
		PGTV	PTVbrain	PTVspine
Average risk	5	50–54	30–30.6	24–30.6
High risk	7	52.2–54.6	30–36.4	30.4–30.6

PTV, planning target volume; PGTV, PTV of gross tumor volume.

instructed to hold breath during CT scanning and maintain the same position as much as possible during magnetic resonance imaging (MRI) scanning. Several lines were marked on the trunk for ensuring the same area for each RT. Plain and enhanced CT images of 3 mm slicing thickness were acquired from above their head to the sacral end for treatment planning using a Siemens Plus 4 Spiral CT system. Then, CT images were imported into the Eclipse TPS (Varian Medical Systems Inc., Version 11.0.31), and the fusion of CT and MRI images was performed for contouring.

Statistical analysis

The paired-samples T-test was used for comparing the treatment techniques, and the results were considered statistically significant when $P \leq 0.05$. All statistical tests were conducted by using SPSS statistical software (Version 22.0).

Radiation planning

IMRT

Designed on the Varian Eclipse TPS with 6 MV photon beams generated by a Varian IX linear accelerator, IMRT plans contained 8 distributed coplanar fields. The position, size, and angle of collimator were adjusted and confirmed by a medical physicist with the same EFFCAST thermoplastic head-neck-shoulder mask. Dose Volume Optimizer (Varian Eclipse, Version 11.0.31) algorithm of Eclipse TPS was utilized for plan optimization. The plans were iteratively optimized by inverse planning software for optimal PTV coverage and OAR sparing. Final dose distribution was calculated by Anisotropic Analytical Algorithm (AAA, Version 11.031) dosage algorithm with a calculation grid size of 2.5 mm.

VMAT

A VMAT plan was optimized by using the progressive resolution of Eclipse TPS (Version 11.0.31), and VMAT repeated the same optimization process as those of the 8F-IMRT plans. Other planning parameters included an MLC motion speed of 0 to 2.5 cm/s, a gantry rotation speed of 0.5 to 4.8 degrees/s and a dosing rate of 0 to 600 MU/min. Final dose distribution was calculated by AAA algorithm with a grid size of 2.5 mm.

HT

HT plans were optimized with TomoTherapy Hi-Art Software (Version 2.0.7) (Accuray, Madison, WI, USA). The operator set the following three major parameters: a field width of 2.5 cm, a pitch of 0.287 and a modulation factor of 2.1–2.6. A collapsed cone convolution model was employed for dose calculations with a grid size of 1.95 mm.

Dose prescription

HT plans were designed by the same experienced medical physicist as the tomotherapy TPS with 6 MV photon beams, and optimized, via least squares optimization containing primary tumor and postoperative residual carcinoma detected by CT/MRI. All gross tumor volume (GTV) images (consisting of tumor bed and residual) were contoured by the same radiologist and confirmed by an experienced radiation oncologist. The clinical target volume (CTV) of the brain included whole brain and CTVspine covered CSF, and spinal canal down to S3. The CTV to PTV margin was 3 mm for the brain and 5 mm for the spine. According to the RTQA Protocol Prescription Guidelines (www.rtog.org), the dose was prescribed to cover 97% of PTV. A volume of at least 0.03 cc within any PTV should not receive >110% of the prescribed treatment. The 0.03 cc volume of overdose for PTV exceeded 110% of the prescribed dose but remained at or below 115%. No volume within PTV 0.03 cc or larger received a dose <93% of its prescribed dose. Any contiguous volume of 0.03 cc or larger of tissue beyond PTV must not receive >110% of dose for primary PTV.

Table 3 Dose constraints for the critical structures and target volumes

Structure	Dose restriction
PTV coverage	
Maximum dose	<110% prescribed dose
Coverage	V100% ≥95% PTV
OARs	
Left lens & right lens planning risk organ volume (PRV)	Max dose <9 Gy
Optic chiasm	Max dose <50 Gy or V54 <1%
Left optic nerve & right optic nerve	Max dose <50 Gy or V54 <1%
Pituitary	Max dose <50 Gy
Brainstem	Max dose <54 Gy
Spinal cord	Max dose <45 Gy
Esophagus	V50 <50%
Heart	V30 <40%
Left lung & right lung	V20 <20%
Liver	V30 <40%
Left kidney & right kidney	V25 <30%
Bowel	Max dose <45 Gy

PTV, planning target volume.

The total prescribed doses of PTV of gross tumor volume (PGTV) were 50–54 Gy, and doses of 30–36.4 Gy were prescribed to PTVbrain and doses of 24–30.6 Gy to PTVspine. The results are summarized in *Table 2*. The lens, brainstem, optic chiasm, optic nerves, pituitary, spinal cord, heart, esophagus, lung, liver, kidneys, and bowels were contoured as OARs. Target dose constraints are summarized in *Table 3*.

Plan evaluations

Dosimetric outcomes of IMRT, VMAT, and HT included PTV and OAR PTV coverage. Target volume coverage, dose homogeneity, and dose conformity were assessed based upon Wu *et al.* (15). Homogeneity index (HI) was defined as follows:

$$HI = (Dmax - Dmin)/Dmean \times 100\%.$$

A value of zero for HI indicated optimal dose homogeneity. That is, higher HI represented worse homogeneous irradiation of PTV.

The equation for the conformal index (CI) is shown below in equation (16):

$$CI = V^2PTV,pres/(VPTV \times Vpres)$$

where VPTV,pres represented the volume of PTV encompassed by 95% isodose volume, VPTV was defined as the volume of PTV or target, and Vpres was total volume receiving dose no lower than prescribed. CI had a range from 0 to 1. The closer the value of CI was to 1, the better conformity of PTV. Dmax, Dmin, and Dmean to PTV and percentage of PTV covered by ≥95% of the prescribed dose (V95%) were also used.

Organs at risk (OARs): Dmax, Dmean and a series of RTOG-recommended values of OARs, including the lenses PRV, optic chiasm, optic nerves, pituitary, brainstem PRV, spinal cord, esophagus, heart, lungs, liver, kidneys, and bowels were analyzed for each patient, with a lower value indicating better protection.

Results

PTV dose coverage and conformality

The dosimetric data and such conformality parameters as Dmax, Dmin, Dmean, CI, V95%, and HI were compared for PTVs. The coverage of PTVs of all three plans was evaluated by comparing target volumes receiving 95% of the prescribed dose (V95%). In PGTV, V95% in IMRT, VMAT and HT were 98.82%±1.76%, 98.07%±1.44% and 99.33%±1.78% respectively; in PTVbrain, V95% were 99.73%±0.51%, 99.93%±0.16% and 99.92%±0.13% in IMRT, VMAT and HT respectively. As for PTVspine, V95% were 99.90%±0.09%, 99.02%±1.38% and 99.96%±0.04% in IMRT, VMAT, and HT respectively. With a similar PTV coverage, all plans fulfilled the prescription requirements and demonstrated an adequate coverage of target volumes.

Comparison of CI and HI in PTVs is shown in *Table 4* and *Figure 1*. PGTV, PTVbrian and PTVspine yielded a similar result of HT plans having the highest conformity, followed by VMAT. CI of PGTV for IMRT, VMAT and HT plans was 0.6096±0.10, 0.6688±0.05 and 0.7163±0.05 respectively; CI of PTVbrain was 0.7815±0.06, 0.8384±0.07 and 0.8490±0.04 respectively; CI of PTVspine was 0.5797±0.08, 0.5862±0.06 and 0.5904±0.04, respectively. Meanwhile, the optimal dose of HI was achieved by HT for PGTV (0.0543±0.02), PTVbrain (0.5525±0.07) and PTVspine (0.0700±0.07). Additionally, IMRT yielded lower HI than VMAT for PGTV (0.0736±0.08 *vs.* 0.0759±0.08) and PTVbrain (0.5554±0.07 *vs.* 0.5619±0.07), and higher HI for PTVspine (0.0877±0.05 *vs.* 0.0782±0.03).

For the same patient, *Figure 2* shows a comparison of

Table 4 Results of dosimetric comparison for PTV ($\overline{X} \pm S$)

PTV	Parameters	IMRT	VMAT	HT	P value		
					IMRT *vs.* VMAT	VMAT *vs.* HT	IMRT *vs.* HT
PGTV	Dmax (Gy)	56.33±2.73	56.76±2.71	56.09±2.38	0.113	0.016	0.302
	Dmin (Gy)	44.68±5.41	44.50±5.53	47.65±4.25	0.622	0.011	0.007
	Dmean (Gy)	54.12±2.14	53.94±2.06	53.93±2.04	0.229	0.902	0.382
	V95%	98.82±1.76	98.07±1.44	99.33±1.78	0.352	0.150	0.688
	CI	0.6096±0.10	0.6688±0.05	0.7163±0.05	0.102	0.027	0.044
	HI	0.0736±0.08	0.0759±0.08	0.0543±0.02	0.500	0.004	0.009
PTVbrian	Dmax (Gy)	56.23±2.73	56.76±2.71	56.09±2.38	0.107	0.015	0.267
	Dmin (Gy)	16.49±7.26	25.01±4.91	25.48±4.81	0.000	0.725	0.001
	Dmean (Gy)	39.32±1.71	38.90±1.87	39.34±2.06	0.008	0.082	0.959
	V95%	99.73±0.51	99.93±0.16	99.92±0.13	0.082	0.974	0.152
	CI	0.7815±0.06	0.8384±0.07	0.8490±0.04	0.007	0.012	0.000
	HI	0.5554±0.07	0.5619±0.07	0.5525±0.07	0.082	0.045	0.036
PTVspine	Dmax (Gy)	44.17±6.76	44.39±7.06	44.92±5.87	0.749	0.021	0.003
	Dmin (Gy)	23.47±3.43	22.01±3.20	24.02±5.26	0.010	0.210	0.934
	Dmean (Gy)	27.83±3.46	27.85±3.55	28.16±3.31	0.820	0.065	0.021
	V95%	99.90±0.09	99.02±1.38	99.96±0.04	0.051	0.039	0.031
	CI	0.5797±0.08	0.5862±0.06	0.5904±0.04	0.756	0.050	0.031
	HI	0.0877±0.05	0.0782±0.03	0.0700±0.07	0.046	0.011	0.029

PTV, planning target volume; IMRT, intensity-modulated radiotherapy; VMAT, volume-modulated arc therapy; HT, helical tomotherapy; CI, conformity index; HI, homogeneity index.

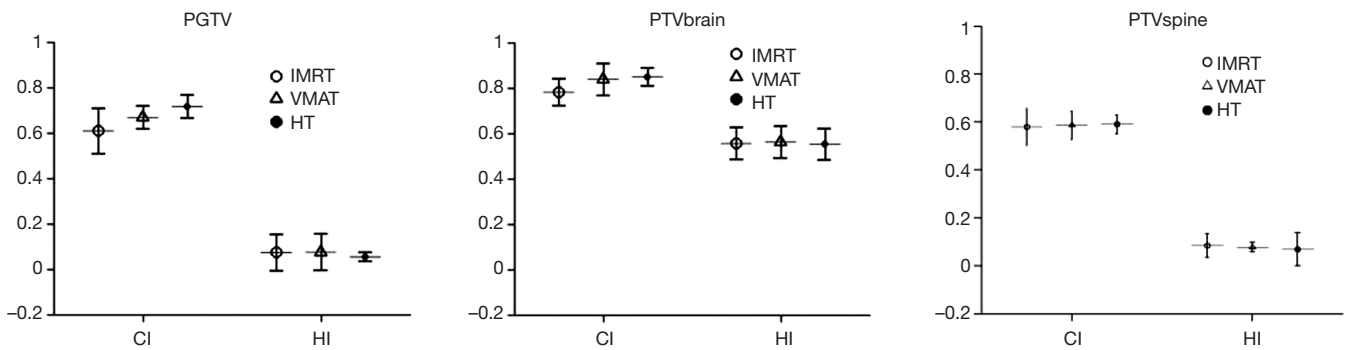

Figure 1 CI and HI of PTVs. CI, conformity index; PTV, planning target volume. HT, helical tomotherapy; IMRT, intensity-modulated radiation therapy; VMAT, volumetric-modulated radiation therapy.

dose distributions for IMRT, VMAT, and HT. Color-washed in the above figure, PTV was 95% covered by 52.2 Gy isodose line (prescribed dose of PGTV) for each technique. Isodose lines of 57.42 Gy (110% prescribed dose), 49.59 Gy (95% prescribed dose), 30 Gy, 20 Gy, and 10 Gy are displayed in *Figure 2*. As expected, dark green (isodose lines of 110% prescribed dose) did not appear in all three plans. Also, the red line (isodose line of

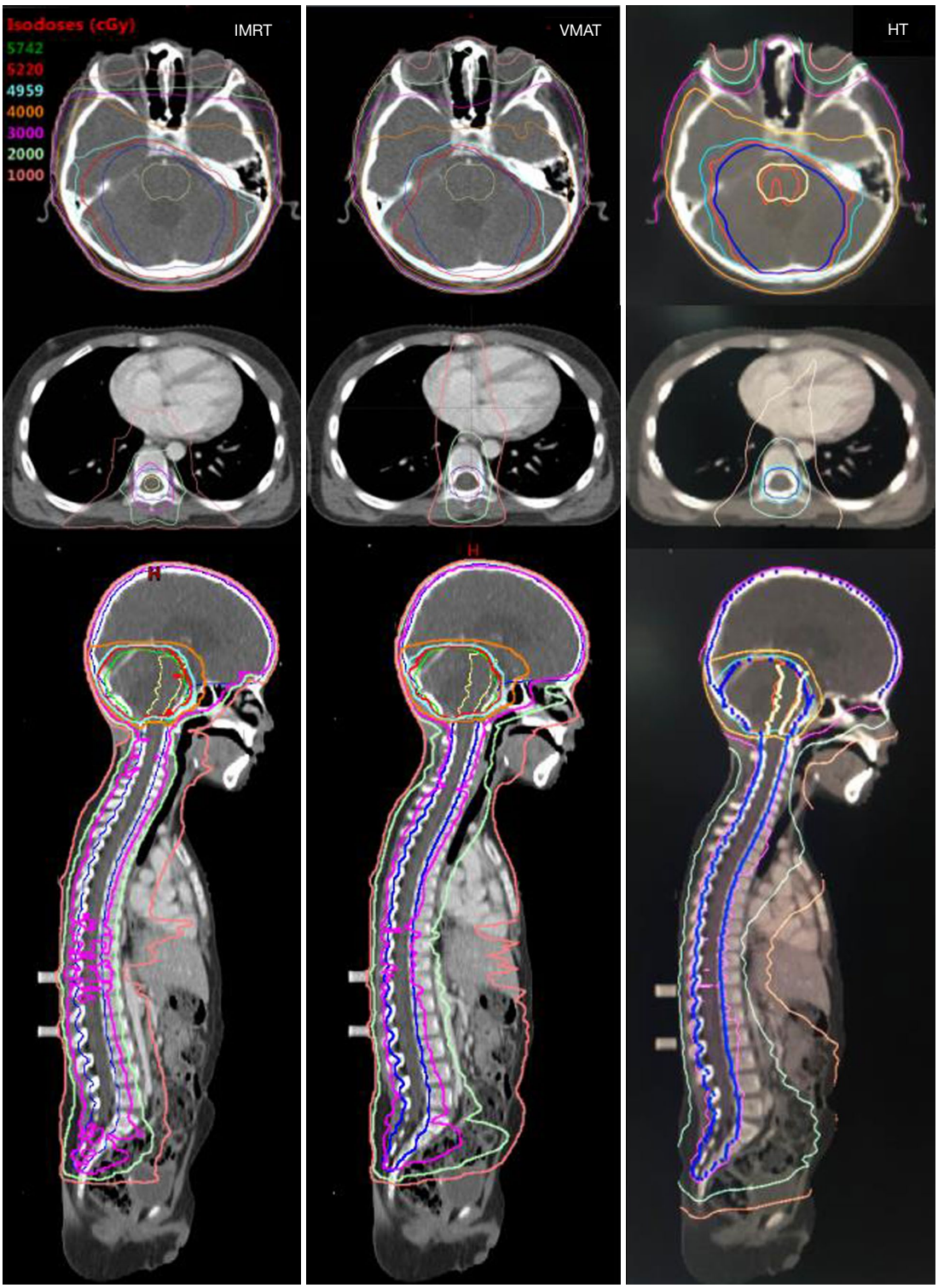

Figure 2 Example dose distribution for the same patient on IMRT, VMAT and HT. Color-wash areas: 57.42 Gy = dark green; 52.20 Gy = red; 49.59 Gy = cyan; 40 Gy = orange; 30 Gy = magenta; 20 Gy = light green; 10 Gy = pink; dark blue line is the outline of PGTV and PTVspine; yellow line is the outline of the brainstem. IMRT, intensity-modulated radiotherapy; VMAT, volume-modulated arc therapy; HT, helical tomotherapy; PTV, planning target volume; PGTV, PTV of gross tumor volume.

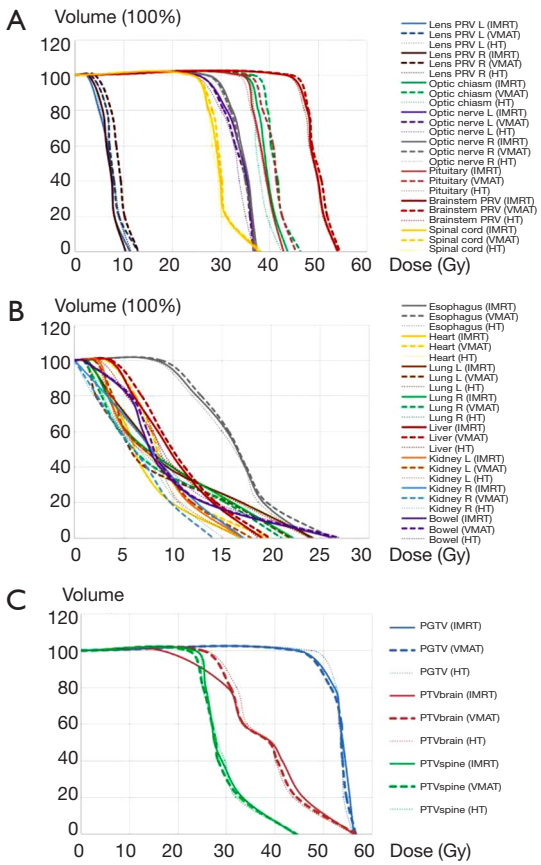

Figure 3 The average DVH to the OARs and PTVs of all patients. (A,B) The average DVH to some selected OARs of the three plan groups; (C) the average DVH for all the PTVs comparing the three plan groups. DVH, dose-volume histogram; OAR, organ at risk; PTV, planning target volume.

52.2 Gy) appeared in brainstem area in HT plan but not in that of IMRT, while VMAT showed that HT had the best protective effect on brainstem among all three methods. The blue lines (isodose lines of PGTV) in IMRT and HT were also entirely encircled by red lines (isodose lines of the prescribed dose) demonstrating good coverage.

OAR sparing

Dose-volume histogram (DVH) for PTVs and selected OARs are presented in *Figure 3*. The doses of D20%, D40%, D60% for OARs were compared for all three plans, and *Table 5* shows a summary of mean and maximal doses to OARs. As compared with VMAT/IMRT, HT lowered the maximal/mean doses of the optic chiasm, brainstem PRV, optic nerves, and bowels. As compared with VMAT/HT, IMRT plans resulted in lower maximal/mean doses for the lens PRV, esophagus and heart. Whereas for lungs and kidneys, VMAT received lower maximal doses than IMRT/HT. There were no statistically significant differences in spinal cord and pituitary live protection.

Discussion

As compared with IMRT/VMAT, HT has been one of the most pressing topics discussed in recent years. Over the last few decades, studies on dosimetric comparing the three radiotherapeutic techniques have shown that dose coverage, conformity/homogeneity of PTV and dose to OARs were satisfactory in all three plans. Despite a longer delivery time, HT has demonstrated improvements of critical avoidance of OARs and target coverage with a highly conformal dose for head-and-neck tumors (17-19). A similar conclusion was drawn from studies on dosimetric comparison among three techniques for tumors in other body parts (20-22). However, few studies have focused upon dosimetric comparisons of various radiation technologies of CSI for medulloblastoma. Existing studies varied greatly in sample size and therapeutic methodology leaving any conclusions made unconvincing. Three methods were exclusively examined, so the present study of comparing IMRT, VMAT and HT plans for CSI is significant. Here, the authors endeavored to offer the overall estimation of dosimetric distribution in three types of treatment plans on the same patient data and provide rationales for selecting optimal plans for medulloblastoma.

The dose distributions of CI and HI in target volume are considered to be the standard parameters of different radiation modalities. The expressions between CI and HI varied in various kinds of literature; however, they shared a similar pattern that a value of CI closer to 1 denoted better conformity and the ideal amount of HI was 0.

Conformity and homogeneity

HT had a prominent characteristic of steep dose gradients with the most substantial V95%, and the optimal CI and the steeper DVH (*Figure 3*). As shown in *Table 4* and *Figure 1*, HT plans had the highest conformity in all PTVs, followed by VMAT ($P<0.05$). The results of our study accorded with other studies indicating better profiles of PTV coverage, CI and HI for HT. In a retrospective dosimetric study, Sharma *et al.* (23) reviewed the CT datasets of 4 pediatric and adolescent female patients

Table 5 Summary of results for the DVH based analysis for OARs ($\overline{X} \pm S$)

OARs	Parameter	IMRT	VMAT	HT	P value		
					IMRT *vs.* VMAT	VMAT *vs.* HT	IMRT *vs.* HT
Left lens PRV	Dmax	11.27±3.27	12.97±2.22	11.60±1.36	0.044	0.008	0.027
	Dmean	6.77±1.65	9.51±1.64	6.93±1.38	0.000	0.003	0.001
Right lens PRV	Dmax	10.45±3.51	13.05±2.50	11.49±1.50	0.001	0.033	0.019
	Dmean	6.63±1.49	9.42±1.53	6.83±1.30	0.000	0.001	0.037
Optic chiasm	Dmax	43.74±5.61	46.45±5.00	42.42±5.90	0.001	0.019	0.009
	Dmean	40.98±4.74	43.64±4.35	40.95±4.49	0.002	0.013	0.004
Left optic nerve	Dmax	37.02±4.28	36.76±0.73	36.08±0.81	0.011	0.016	0.045
	Dmean	32.70±2.89	31.34±1.57	31.20±0.82	0.059	0.025	0.029
Right optic nerve	Dmax	37.47±3.05	36.80±1.96	36.74±3.13	0.040	0.039	0.024
	Dmean	34.70±4.80	31.72±1.82	31.22±1.41	0.002	0.008	0.049
Pituitary	Dmax	42.62±6.28	45.43±4.93	42.79±5.37	0.091	0.006	0.151
	Dmean	40.92±5.49	43.39±4.22	40.75±4.81	0.027	0.004	0.362
Brainstem PRV	Dmax	54.04±1.53	54.45±1.64	53.86±1.42	0.176	0.036	0.027
	Dmean	48.95±2.98	49.61±2.39	48.77±2.68	0.050	0.042	0.037
Spinal cord	Dmax	37.82±2.37	38.20±2.86	41.54±3.24	0.151	0.010	0.054
	Dmean	30.00±4.04	29.80±3.65	29.39±2.86	0.087	0.103	0.052
Esophagus	Dmax	24.07±4.49	26.21±3.83	24.18±4.38	0.006	0.829	0.022
	Dmean	15.05±3.03	18.95±3.44	18.51±4.09	0.000	0.393	0.001
Heart	Dmax	16.03±3.37	19.68±3.06	19.42±3.98	0.000	0.777	0.002
	Dmean	5.90±1.52	8.49±1.53	8.41±1.93	0.000	0.870	0.000
Left lung	Dmax	23.30±3.75	21.97±4.68	23.93±3.22	0.053	0.005	0.112
	Dmean	5.27±0.92	3.40±0.98	4.12±1.10	0.000	0.028	0.000
Right lung	Dmax	23.90±3.76	22.98±3.42	25.14±2.71	0.056	0.000	0.023
	Dmean	5.69±0.89	4.39±0.95	5.05±1.13	0.000	0.016	0.007
Liver	Dmax	19.09±5.04	19.87±3.60	18.73±3.60	0.047	0.164	0.641
	Dmean	5.38±0.83	5.62±0.73	5.02±0.42	0.257	0.001	0.383
Left kidney	Dmax	17.13±4.83	14.21±3.60	16.72±3.81	0.001	0.003	0.624
	Dmean	5.54±1.89	2.91±0.87	3.91±1.35	0.000	0.000	0.001
Right kidney	Dmax	17.22±5.05	14.11±3.61	15.13±4.06	0.000	0.028	0.166
	Dmean	5.48±2.05	2.75±1.25	3.70±1.32	0.000	0.003	0.000
Bowel	Dmax	26.32±4.21	26.99±4.41	25.38±3.69	0.009	0.007	0.026
	Dmean	6.07±1.58	7.25±1.62	8.17±180	0.000	0.021	0.000

DVH, dose-volume histogram; OAR, organ at risk; PRV, planning risk organ volume; IMRT, intensity-modulated radiotherapy; VMAT, volume-modulated arc therapy; HT, helical tomotherapy.

(mean age, 9 years; range, 5–14 years). The optimal dose CI was achieved by HT for PTVbrain (0.96) and IMRT_LA for PTVspine (0.83). HT appeared to be ideally suited for long and complex-shaped target volumes and avoided any junction, field-matching, and abutment dosimetry. In another study reported by Zong-Wen *et al.* (24), 5 adult medulloblastoma patients confirmed pathologically and receiving HT were enrolled for dosimetric comparison of CSI treatments using HT, VMAT and three-dimensional CRT (3DCRT). The doses for PTV1 (brain & spinal cord) and PTV2 (posterior cranial fossa) were 30.6–36 Gy/17–20 F and 50.4–54 Gy/28–30 F respectively. The lowest mean dose homogeneity index (DHI) (DHI = D5%/D95%) indicated the best homogeneity of the target for HT plans comparing VMAT and 3DCRT (1.05 *vs.* 1.07 & 1.09), and the target volume exposed to high dose (V107%) in VMAT was more significant than that of HT. Moreover, HT provided the best conformity with a mean CI of 0.87. Meanwhile, the poorest dose conformation to the target volume (mean CI =0.69) was observed with 3DCRT. Other studies of dosimetric comparison of head-and-neck tumor have reached the same conclusion. As reported by Chen *et al.* (25), 30 locally advanced NPC patients were selected for IMRT, VMAT and HT to evaluate the potential dosimetric gains of HI and CI of PTVs. It turned out that HT offered significantly improved target dose conformity. In another study of Skórska *et al.*'s (26), a total of 45 treatment plans were calculated retrospectively for 15 cases of brain tumors. The dosimetric comparison was made for HT versus coplanar (cIMRT) and non-coplanar (n-cIMRT) beam arrangements, and median HI and CI were the best for HT plans and the worst for cIMRT.

As shown in *Table 4* and *Figure 1*, HT showed superior dose homogeneity in PTVs as compared with IMRT/VMAT (P<0.05). Similar conclusions were drawn from the studies of other head and neck tumors. Liu *et al.* (27) reported that HT was preferred in terms of dose homogeneity as compared with VMAT, IMRT and 3D-CRT (P<0.05) in stage I–II nasal natural killer/T-cell lymphoma (NNKTL). For PTV-spine, HT achieved the highest mean DHI of 0.96 as compared with 0.91 for IMRT LA and 0.84 for 3DCRT. van Vulpen *et al.* (28) conducted a dosimetric comparison of HT, and coplanar LINAC-based IMRT for oropharyngeal carcinoma and HT provided improved dose homogeneity. For nasal cavity and paranasal sinus tumors receiving n-cIMRT, Sheng *et al.* (29) examined the dosimetric differences between non-coplanar IMRT *vs.* HT. Uniformity index (UI) (UI = D5/D95 where D5 and D95 were minimal doses delivered to 5% and 95% of PTV) was used to assess the uniformity of both plans. HT DVH had a steeper slope and lowered UIs indicating a higher consistency within PTV. Borghetti *et al.* (30) compared VMAT/HT with adjuvant stereotactic boost (SRS) or simultaneous integrated boost (SIB) for brain metastasis; SRS plans showed that HI was 0.07 for both techniques (quite close to optimal). For SIB plans, HI was 0.03 and 0.08 for HT and VMAT respectively. This suggests that HT-SIB could deliver slightly better plans than VMAT-SIB.

OARs

The three plans all demonstrated positive and negative properties in OAR protection. Maximal/mean doses of lungs and kidneys in VMAT plan were lower than in IMRT and HT (P<0.05). Meanwhile, IMRT fared better in maximal/mean doses of OARs close to mid-body, including esophagus and heart than VMAT and HT (P<0.05). However, HT was superior for critical organs including maximal/mean doses of brainstem PRV (P<0.05), optical chiasm (P<0.05) and optic nerves (P<0.05) than IMRT and VMAT.

As discussed by Kissick *et al.* (31), fixed field size during dose delivery and a lack of second pair of MLC caused HT to deliver a relatively larger "dose spread" in the superior-inferior direction. Also, complete target coverage in the superior-inferior direction could be achieved only by opening and closing the field to an approximately half-field width superior to the cranial end of the target and inferior to the caudal end of the goal. It directly contributed to dose elevation in superior and inferior OARs immediately adjacent to the target, such as a higher dose of the lens in HT than IMRT (*Table 5*).

Several dosimetric studies of head & neck tumors reported that HT was superior in protecting brainstem, optical chiasm, and optic nerves. As reported by Skórska *et al.* (26), the lowest mean dose to the brainstem, optical chiasm, and ipsilateral optic nerve was achieved for HT when compared with n-cIMRT and cIMRT plans in a diverse group of brain tumors. In the SRS cases presented by Borghetti *et al.* (30), there was no statistical difference in OARs between VMAT and helical IMRT, but HT was generally better in terms of maximal doses, particularly for the optic chiasm (30.31 *vs.* 32.36 Gy; P=0.002) and brainstem (30.95 *vs.* 33.11 Gy; P=0.013) than VMAT in SIB cases in the treatment of brain metastasis in RPA classes I-II patients. Our study was almost consistent with

the ones reported above. Still, there were certainly some differing points. A slight discrepancy might be caused by: (I) differences in contouring targets and OARs; (II) fan beam thicknesses, pitch and modulation factors used as optimization parameters; (III) location and quantity of directional blocks; and (IV) number of patients.

The feasibility of IMRT was properly evaluated. However, long-term follow-ups of acute toxicity treated with two other techniques should be compared with the more significant number of patients. Schiopu *et al.* (32) described early/late toxicity, survival and local control in 45 CNS tumor patients on HT. The most common acute toxicities were nausea, vomiting, fatigue, loss of appetite, alopecia, and neurotoxicity. The 3- and 5-year survival rates were 80% and 70% respectively—one case developed secondary cancer. As reported by Sugie *et al.* (33), CSI was offered for 6 children aged under 13 years and 6 adults. There were severe hematological toxicities for HT. Thus, HT might increase the possibility of exposing larger volumes of normal tissues to lower radiation doses (34). It has become a serious concern of secondary malignancies. Improving the defects of those photon-based techniques, like proton beam treatment (PBT), because of the advantageous Bragg-peak physical properties of a near-zero exit or distal dose just beyond the target volume, was expected to be the ideal treatment. A study of Yoon *et al.* (35), from the Proton Therapy Center of National Cancer Center, showed PBT had an advantage in the average OAR doses for the chest and abdomen region when compared with CRT (3D-CRT) and HT. Howell *et al.* (36) also found PBT allowed for a statistically significant reduction in normal tissues in OARs across a wide age and BMI spectrum while providing more homogeneous coverage than that of photon CSI. Further study (37) including the advantages of utilizing compensator in PBT for the whole brain as a component of CSI, optimization of a rotating bracket in PBT, etc., is necessary in order to find the best mode of PBT. In short, when considering clinical practice, one must weigh the theoretical risk of acute toxicity and long-term effects, including secondary malignancies, with other benefits in dose distribution for individualized optimal plans.

Conclusions

For CSI, IMRT, HT, and VMAT all showed excellent target coverage. However, the use of HT showed improvements in CI and HI, resulting in better sparing of brainstem PRV, optical chiasm, and optic nerves. The incidence and severity between the acute toxic reaction and the late sequels are somewhat less definite for the three radiotherapeutic techniques. Therefore, future clinical studies with longer follow-ups are recommended. Thus proper usage and individualized choice of methods are of vital importance.

Acknowledgments

Funding: This work was supported by a grant of the Department of Science and Technology of Hunan province of China (No. 2017SK50105), and a grant of the Changsha City Science & Technology Bureau (kq1701095), China.

Footnote

Conflicts of Interest: All authors have completed the ICMJE uniform disclosure form (available at http://dx.doi.org/10.21037/tcr.2019.01.30). The authors have no conflicts of interest to declare.

Ethical Statement: The authors are accountable for all aspects of the work in ensuring that questions related to the accuracy or integrity of any part of the work are appropriately investigated and resolved. The study is retrospective and does not involve the treatment of patients. The study protocols were approved by the Ethical Committee of the Xiangya Hospital of Central South University (No. 2017121010).

References

1. Polkinghorn WR, Tarbell NJ. Medulloblastoma: tumorigenesis, current clinical paradigm and efforts to improve risk stratification. Nat Clin Pract Oncol 2007;4:295-304.
2. Christine Fuller. WHO Classification of Tumours of the Central Nervous System, Fourth Edition. J Neuropathol Exp Neurol 2008;67:260.

3. Newbold K, Partridge M, Cook G, et al. Advanced imaging applied to radiotherapy planning in head and neck cancer: a clinical review. Br J Radiol 2006;79:554-61.
4. Thwaites DI, Tuohy JB. Back to the future: the history and development of the clinical linear accelerator. Phys Med Biol 2006;51:R343-62.
5. Spirou SV, Chui CS. A gradient inverse planning algorithm with dose-volume constraints. Med Phys 1998;25:321-33.
6. Xie X, Ouyang S, Wang H, et al. Dosimetric comparison of left-sided whole breast irradiation with 3D-CRT, IP-IMRT and hybrid IMRT. Oncol Rep 2014;31:2195-205.
7. Sun X, Su S, Chen C, et al. Long-term outcomes of intensity-modulated radiotherapy for 868 patients with nasopharyngeal carcinoma: an analysis of survival and treatment toxicities. Radiother Oncol 2014;110:398-403.
8. Zhou Q, He Y, Zhao Y, et al. A study of 358 cases of locally advanced nasopharyngeal carcinoma receiving intensity-modulated radiation therapy: Improving the Seventh Edition of the American Joint Committee on Cancer T-Staging System. Biomed Res Int 2017;2017:1419676.
9. Kuang WL, Zhou Q, Shen LF. Outcomes and prognostic factors of conformal radiotherapy versus intensity-modulated radiotherapy for nasopharyngeal carcinoma. Clin Transl Oncol 2012;14:783-90.
10. Wang W, Yang H, Mi Y, et al. Rules of parotid gland dose variations and shift during intensity modulated radiation therapy for nasopharyngeal carcinoma. Radiat Oncol 2015;10:3.
11. Su J, Chen W, Yang H, et al. Different setup errors assessed by weekly cone-beam computed tomography on different registration in nasopharyngeal carcinoma treated with intensity-modulated radiation therapy. Onco Targets Ther 2015;8:2545-53.
12. Mansur DB, Klein EE, Maserang BP. Measured peripheral dose in pediatric radiation therapy: a comparison of intensity-modulated and conformal techniques. Radiother Oncol 2007;82:179-84.
13. Lee YK, Brooks CJ, Bedford JL, et al. Development and evaluation of multiple isocentric volumetric modulated arc therapy technique for craniospinal axis radiotherapy planning. Int J Radiat Oncol Biol Phys 2012;82:1006-12.
14. Palma DA, Verbakel WF, Otto K, et al. New developments in arc radiation therapy: a review. Cancer Treat Rev 2010;36:393-9.
15. Wu Q, Mohan R, Morris M, et al. Simultaneous integrated boost intensity-modulated radiotherapy for locally advanced head-and-neck squamous cell carcinomas. I: Dosimetric results. Int J Radiat Oncol Biol Phys 2003;56:573-85.
16. van't Riet A. A conformation number to quantify the degree of conformality in brachytherapy and external beam irradiation: application to the prostate. Int J Radiat Oncol Biol Phys 1997;37:731.
17. Peters S, Schiefer H, Plasswilm L. A treatment planning study comparing Elekta VMAT and fixed field IMRT using the Varian treatment planning system eclipse. Radiat Oncol 2014;9:153.
18. Stieler F, Wolff D, Schmid H, et al. A comparison of several modulated radiotherapy techniques for head and neck cancer and dosimetric validation of VMAT. Radiother Oncol 2011;101:388-93.
19. Lu SH, Cheng JC, Kuo SH, et al. Volumetric modulated arc therapy for nasopharyngeal carcinoma: a dosimetric comparison with tomotherapy and step-and-shoot IMRT. Radiother Oncol 2012;104:324-30.
20. McGrath SD, Matuszak MM, Yan D, et al. Volumetric modulated arc therapy for delivery of hypofractionated stereotactic lung radiotherapy: a dosimetric and treatment efficiency analysis. Radiother Oncol 2010;95:153-7.
21. Moon SH, Shin KH, Kim TH, et al. Dosimetric comparison of four different external beam partial breast irradiation techniques: three-dimensional conformal radiotherapy, intensity-modulated radiotherapy, helical tomotherapy, and proton beam therapy. Radiother Oncol 2009;90:66-73.
22. Palma D, Vollans E, James K, et al. Volumetric modulated arc therapy for delivery of prostate radiotherapy: comparison with intensity-modulated radiotherapy and three-dimensional conformal radiotherapy. Int J Radiat Oncol Biol Phys 2008;72:996-1001.
23. Sharma D S, Gupta T, Jalali R, et al. High-precision radiotherapy for craniospinal irradiation: evaluation of three-dimensional conformal radiotherapy, intensity-modulated radiation therapy and helical TomoTherapy. Br J Radiol 2009;82:1000-9.
24. Zong-Wen S, Shuang-Yan Y, Feng-Lei D, et al. Radiotherapy for adult medulloblastoma: evaluation of helical tomotherapy, volumetric intensity modulated arc therapy, and three-dimensional conformal radiotherapy and the results of helical tomotherapy therapy. Biomed Res Int 2018;2018:9153496.
25. Chen W, Yang X, Jiang N, et al. Intensity-modulated radiotherapy, volume-modulated arc therapy and helical tomotherapy for locally advanced nasopharyngeal carcinoma: a dosimetric comparison. Transl Cancer Res 2017;6:929-39.

26. Skórska M, Piotrowski T, Kazmierska J, et al. A dosimetric comparison of IMRT versus helical tomotherapy for brain tumors. Physica Medica 2014;30:497-502.
27. Liu X, Huang E, Ying W, et al. Dosimetric comparison of helical tomotherapy, VMAT, fixed-field IMRT and 3D-conformal radiotherapy for stage I-II nasal natural killer T-cell lymphoma. Radiat Oncol 2017;12:76.
28. van Vulpen M, Field C, Cornelis PJ, et al. Comparing step-and-shoot IMRT with dynamic helical tomotherapy IMRT plans for head-and-neck cancer. Int J Radiat Oncol Biol Phys 2005;62:1535-9.
29. Sheng K, Molloy JA, Larner JM, et al. A dosimetric comparison of non-coplanar IMRT versus helical tomotherapy for nasal cavity and paranasal sinus cancer. Radiother Oncol 2007;82:174-8.
30. Borghetti P, Pedretti S, Spiazzi L, et al. Whole brain radiotherapy with adjuvant or concomitant boost in brain metastasis: dosimetric comparison between helical and volumetric IMRT technique. Radiat Oncol 2016;11:59.
31. Kissick MW, Flynn RT, Westerly DC, et al. On the making of sharp longitudinal dose profiles with helical tomotherapy. Phys Med Biol 2007;52:6497-510.
32. Schiopu SR, Habl G, Häfner M, et al. Craniospinal irradiation using helical tomotherapy for central nervous system tumors. J Radiat Res 2017;58:238-46.
33. Sugie C, Shibamoto Y, Ayakawa S, et al. Craniospinal irradiation using helical tomotherapy: evaluation of acute toxicity and dose distribution. Technol Cancer Res Treat 2011;10:187-95.
34. Pai Panandiker A, Ning H, Likhacheva A, et al. Craniospinal irradiation with spinal IMRT to improve target homogeneity. Int J Radiat Oncol Biol Phys 2007;68:1402.
35. Yoon M, Shin DH, Kim J, et al. Craniospinal Irradiation Techniques: A Dosimetric Comparison of Proton Beams With Standard and Advanced Photon Radiotherapy. Int J Radiat Oncol Biol Phys 2011;81:637-46.
36. Howell RM, Giebeler A, Koontzraisig W, et al. Comparison of therapeutic dosimetric data from passively scattered proton and photon craniospinal irradiations for medulloblastoma. Radiat Oncol 2012;7:116.
37. Dinh J, Stoker J, Georges RH, et al. Comparison of proton therapy techniques for treatment of the whole brain as a component of craniospinal radiation. Radiat Oncol 2013;8:289.

Cite this article as: Sun Y, Liu G, Chen W, Chen T, Liu P, Zeng Q, Hong J, Wei R. Dosimetric comparisons of craniospinal axis irradiation using helical tomotherapy, volume-modulated arc therapy and intensity-modulated radiotherapy for medulloblastoma. Transl Cancer Res 2019;8(1):191-202. doi: 10.21037/tcr.2019.01.30

